Darwin's entangled bank through deep time: Structural stability of mutualistic networks over large geographic and temporal scales

Benoît Perez-Lamarque[1], Jérémy Andréoletti[2], Baptiste Morillon[2], Orane Pion-Piola[2], Amaury Lambert[2], and Hélène Morlon[2]

[1] Université de Toulouse, Toulouse INP, CNRS, IRD, CRBE, Toulouse, France
[2] Institut de biologie de l'École normale supérieure (IBENS), École normale supérieure, CNRS, INSERM, Université PSL, 46 rue d'Ulm, 75 005 Paris, France

*corresponding author: benoit.perez-lamarque@utoulouse.fr; ORCID: 0000-0001-7112-7197

Author Contributions:
All authors designed this study. BPL performed the analyses. BPL and HM analyzed the data and wrote the first version of the manuscript and all authors contributed to the revisions.

Competing Interest Statement:
The authors declare no conflict of interests.

Keywords: species interactions, macroevolution, bipartite network, plant mutualism, latent trait, Brownian motion.

Abstract:

Mutualistic interactions form species-rich, complex networks that play essential roles for ecosystem function. Over macroevolutionary time scales, global- and continental-level networks change as species emerge and go extinct, yet the stability of their structural organization remains poorly understood. Here, we show that ancestral interaction networks can be reconstructed from present-day phylogenetic and interaction data. We infer the ancestral networks of plant mutualisms involving arbuscular mycorrhizal fungi, bat pollinators, and bird seed dispersers at large biogeographic scales. We find that these mutualistic networks exhibit a modular structure that has persisted for millions of years, maintained by the evolutionary conservatism of species interactions. As species diversify, they show limited shifts in mutualistic partners. This minimal evolutionary rewiring results in a remarkable long-term stability of mutualistic network structure at large spatial scales.

Introduction:

Mutualistic interactions play a key role in ecosystems (1), and have also been central to the evolution of life on Earth (2, 3). Species involved in mutualistic interactions are interconnected through shared partners, forming complex bipartite interaction networks (4). The structure of these networks is typically non-random, often displaying nestedness – where specialist species preferentially interact with generalists, or modularity, in which distinct subsets of species interact more frequently among themselves than with species outside their group (5–7). In some cases, both patterns can be present simultaneously (8, 9). Historically, research has focused on local, community-scale networks, revealing that non-random structures can influence community stability. More recently, networks compiled at regional to global scales have revealed a tendency toward modularity (10). However, this tendency is not universal (11, 12), and its underlying causes remain poorly understood.

Present-day networks at regional to global scales result from ecological and evolutionary processes operating over millions of years (6, 13). Fundamental yet unresolved questions include when their structural organization emerged, what processes shaped it, and whether these structures are evolutionary stable (14–16). If species distributions tend to be restricted to specific biogeographic areas, for example due to dispersal limitation or ecological filtering, we may expect the formation of stable modules aligned with biogeographic regions (10). Likewise, if mutualistic interactions are largely conserved as species diversify, we may expect the formation of stable modules composed of closely-related species (17). Conversely, if a significant fraction of species is ubiquitous and mutualistic interactions are more evolutionarily labile, large-scale networks may be more nested, a structure that enhances robustness to species extinctions (5).

The degree to which species biogeographic distributions are restricted, and mutualistic interactions evolutionary conserved, is therefore expected to have important implications for network structure at large spatial scales. Species distributions depend mostly on the dispersal capacity and niche breath of species. Periods of environmental stability may favor ecological specialization, which may reduce niche breadth and favor modular structures. As for the phylogenetic conservatism in interaction partners, we may expect selection to favor the retention of existing beneficial associations (18). Coevolution may then reinforce reciprocal specialization and compartmentalization (19). However, several processes can

counteract this stabilizing selective force, favoring partner shift and reducing phylogenetic conservatism. These include opposing selective pressures during periods of environmental instability, competition for shared partners between closely-related species (20), pairwise coevolution across geographically distinct regions resulting in independent local adaptations (21), and the exploitation of mutualism by cheaters, which can destabilize mutualistic interactions (22). Indeed, empirical evidence for phylogenetic conservatism of mutualistic interactions is mixed (23).

Hypotheses on the emergence and evolutionary stability of network structures are particularly challenging to test. Indeed, direct observation of the fossil record is limited by both low taxonomic resolution and a lack of evidence with respect to the interactions. Only a few networks have been reconstructed from fossil deposits (24, 25), and these primarily represent trophic interactions, which leave more readily interpretable evidence than mutualistic ones. An alternative is to reconstruct ancestral networks (i.e., probable ancestral interactions) using knowledge of present-day interactions and phylogenetic relationships. Inspired by models of historical biogeography (26), Braga *et al.* (27) developed a probabilistic model for the evolution of host repertoire (*i.e.* the set of hosts a species interacts with) along a phylogeny that allows reconstructing ancestral host repertoires (27, 28). However, this approach is computationally costly, hampering a fine-grained characterization of ancestral network structure, particularly at large biogeographic scales.

Here, we begin by developing an efficient method to reconstruct ancestral networks, based on the idea that interactions are shaped by unobserved traits evolving over the course of history (29, 30). We then apply this approach to four large scale networks of plant mutualisms. For hundreds of millions of years, plants have engaged in diverse and persistent mutualistic interactions with animals and microorganisms, which play crucial roles in their nutrition, protection and reproduction (31–33). We reconstruct ancestral mutualistic networks of plants with arbuscular mycorrhizal fungi at the global scale over the past 150 Myr, bat pollinators in the Neotropics over the past 12 Myr, and bird seed dispersers in Europe and in the Americas over the past 10 Myr, and track how their structure changes through time.

Results:

We developed the "Evolution of LatEnt traits For Ancestral NeTwork reconstruction" model (ELEFANT, Figure 1, see Methods). We assume that interspecific interactions are shaped by species-specific traits, such as the production and detection of floral scents, or the morphological complementarity of spur and proboscis lengths in pollination systems. However, such traits are often unknown and/or difficult to measure in most empirical systems. Thus, instead of relying on directly measured traits, ELEFANT infers unobserved "latent" traits from the present-day interaction matrix, using singular value decomposition (29, 30) (see Methods ; Figure 1.1). By construction, each species is represented by a vector of several latent trait values, and the interaction probability between a pair of species is determined by the product of their corresponding latent trait values. This interaction rule does not match classical formulations of trait matching (as, for example in (6, 34)), yet as we will show, it is effective in representing who interacts with whom. Next, we "augment" the phylogenetic trees associated with the present-day interaction network in order to account for lineages that are, or were, likely involved in the system considered (e.g., bird seed dispersers in Europe over the past 10 Myr) but are not represented in the trees, because they went extinct or were not sampled (Figure 1.2). If diversification occurs *in situ* at the spatial scale of the network, as in large (continental to global scale) networks over sufficiently short timescales, or in close communities of *in situ* radiations, such as those found on remote islands or lakes, this can be done by assuming that clades evolve according to a birth-death process representing speciation and extinction events, using data augmentation to obtain "complete" trees with probable configurations of missing lineages (35). Finally, as in (30), we assume that the latent traits evolve according to traditional phylogenetic models of trait evolution, such as the Brownian motion process. We use ancestral trait reconstruction to infer latent trait values along the augmented phylogenies (30, 36)(Fig. 1.3), and deduce ancestral networks (Figure 1.4). Like any model, ELEFANT relies on strong assumptions, and *at a minimum,* requires interactions to be evolutionary conserved to some extent. This condition may not always be met; therefore, the final step of our procedure is specifically designed to assess whether the model can be reliably applied to the network under investigation (Figure 1.5). The principle of this "cross-validation" procedure is to assess the ability of the model to recover known interactions. Specifically, we artificially remove (subsample) a given percentage of present-day species, estimate the latent traits using the network formed by the remaining species, and then reconstruct these traits along the complete phylogeny, including at present

for the subsampled species. From these reconstructions, we infer the interactions of the subsampled species. Comparing the inferred interactions with the known ("true") ones yields a cross-validation (F1) score. Low scores indicate that the data violate one or more model assumptions (e.g., Brownian evolution of latent traits) and, consequently, that the model should not be used to infer ancestral networks.

Figure 1: General framework used to reconstruct ancestral networks

The Evolution of LatEnt traits for Ancestral Network reconsTruction framework (ELEFANT), proceeds in five steps. 1) Given a bipartite interaction network (N), a vector of d latent trait values is estimated for each extant species on each side of the network; these vectors (compiled into matrices $\tilde{L}$ and $\tilde{R}$) underlie present-day interactions (for clarity only the first latent trait value is represented here with the color code). 2) Data augmentation is used to add extinct and unsampled lineages (colored in green) on the phylogenetic trees, assuming constant rates of speciation (λ), extinction (μ), and sampling at present (ρ). 3) Ancestral values of the latent traits are estimated on the two phylogenetic trees using Brownian motion. 4) Ancestral interaction networks are reconstructed from the estimated ancestral latent trait values at any time in the past (e.g. here, 50 Mya) 5) A cross-validation procedure based on the ability to recover known interactions at present in a specific system provides a measure of confidence.

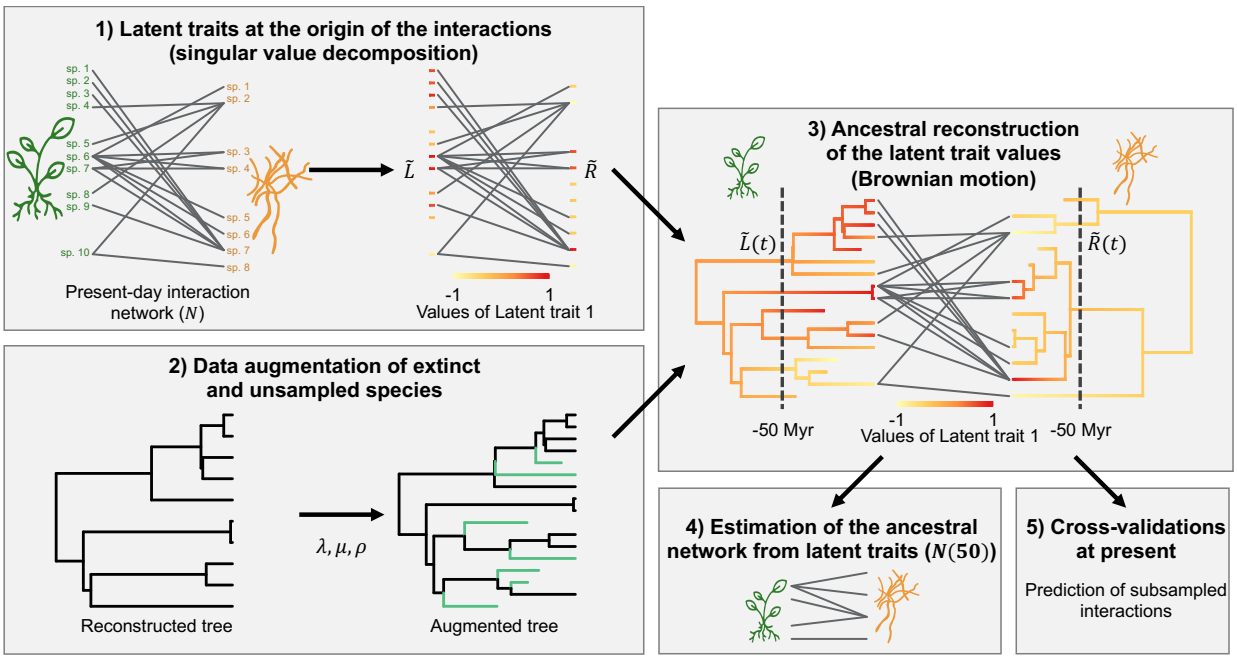

We thoroughly tested the ability of ELEFANT to reconstruct ancestral interaction networks using simulated data. We mimicked 30 Myr of network evolution during the diversification of two interacting guilds (hereafter referred to as "plants" and "mutualists" for simplicity, but ELEFANT can be applied to any type of bipartite network, including antagonistic ones) under five distinct scenarios (see Methods): i) The first scenario ("evolution by anagenetic shifts") considers that interactions are inherited at speciation, but can change during a species' lifespan. ii) The second scenario ("evolution by cladogenetic shifts") adds the occurrence of cladogenetic shifts, where upon speciation of a mutualist species, one of the daughter lineages retains its plant partners, while the other forms an entirely new set of interactions with randomly selected plant species. iii) The third scenario (" Brownian evolution of latent traits") corresponds to the model underlying ELEFANT, where traits evolve as Brownian processes on the plant and mutualist phylogenies and their products determine whether species interact. iv) In the fourth scenario ("host repertoire evolution"), inspired from Braga *et al.* (27), host repertoires (i.e. the plant lineages that a mutualist interacts with) are fixed while mutualists diversify, for example corresponding to higher taxonomic levels; host repertoires are inherited upon the speciation of mutualists, and they can be acquired or lost during the lifespan of a mutualist. v) Finally, the fifth scenario ("random evolution") mimics very frequent anagenetic shifts. In scenarios i), iii) and iv) interspecific interactions tend to be conserved over macroevolutionary timescales, while in scenarios ii) and v) they are more labile. We applied ELEFANT to these simulated data and computed cross-validation scores (i.e., F1-scores at present). In addition, to assess the robustness of our reconstructions, we computed F1-scores from ancestral networks.

We found that our cross-validation procedure effectively discriminates between cases in which ancestral networks can be robustly reconstructed—at least in the recent past (scenarios i, iii, and iv, characterized by conserved interactions)—and cases in which they cannot (scenarios ii and v, characterized by evolutionary labile interactions) (Fig. S1 & S2). Cross-validation scores are above 0.75 for scenario i), and above 0.5 for scenarios iii) and iv), but around 0.20 for scenario ii) and below 0.10 for scenario v) (Fig. S1). The ability to recover correct ancestral interactions (F1-scores from ancestral networks) is well correlated with the F1-scores of the cross-validations at present (Fig. S2). In the recent past, the F1-scores of ancestral reconstructions are in fact higher than the cross-validation score: a cross-validation score above 0.25 typically indicates that the inferred ancestral interactions are likely to be correct (F1-score >0.5), suggesting 0.25 as a good operational minimum threshold for the application of ELEFANT to a

given empirical system. When interactions are not too labile, which in practice is reflected by a F1-score above 0.25, ancestral interactions are well recovered, in particular in the recent past (Figs. 2 and S3). It follows that global metrics (connectance – *i.e.* the ratio of realized interactions –, nestedness, and modularity) and phylogenetic signal in species interactions are also well recovered, although with a tendency toward homogenization (*i.e.* the lowest and highest simulated metrics tend to be estimated closer to the average; Figs. 2, S4 & S5). The estimations of global metrics are particularly precise close to the present (5 Myr ago: mean R^2=0.79) and become noisier back in the past (20 Myr ago: mean R^2=0.32), with a good recovery of temporal trends (see Supplementary results; Fig. S6). These results suggest to be careful with the interpretation of ancestral networks constructed past halfway through the clades' age.

Confident in our framework, we inferred the ancestral networks for four large plant-mutualist systems (see Methods): i) the global-scale mutualism with arbuscular mycorrhizal fungi (115 plant families and 351 fungal taxa over the past 150 Myr), ii) interactions with bat pollinators in the Neotropics (42 plant families and 56 bat species over the past 12 Myr), iii) bird-mediated seed dispersal in Europe (28 plant families and 70 bird species over the past 10 Myr), and iv) bird-mediated seed dispersal in the Americas (115 plant families and 586 bird species over the past 10 Myr). Cross-validation F1-scores were all above 0.25 (0.32, 0.27, 0.70, and 0.46 for i), ii), iii) and iv) respectively), indicating the validity of using our approach. Our reconstructions reveal a strikingly consistent pattern of modularity across the four systems, despite variation in species richness and composition over time (Figs. 3, 4 & 5). Plant degrees (*i.e.,* the mean number of partners per species) tend to be lower than expected under null models in three of the four systems (significantly so in two), reflecting a tendency toward specialization. Species interactions appear to be generally evolutionarily conserved (significant phylogenetic signal except in the smaller size European bird dispersal network, Figs. 3, 4 & 5). These results are robust to diversification rates and sampling fractions used to augment the trees (Fig. S7). They suggest a scenario where mutualistic associations are evolutionary conserved, favoring specialization and resulting in the formation of stable modules, where closely-related taxa interact with closely-related partners.

Figure 2: Accurate reconstruction of ancestral networks

A: Bar charts indicate the F1-score (blue), the proportion of false positives (red), and the proportion of recovered interactions (green) inferred in the cross-validations at present (upper row) and in the consensus ancestral networks (from 5 to 30 Myr ago; lower rows). 30 Mya corresponds to the most recent common ancestor of the mutualists, which interacted with a single plant species. These consensus networks assemble interactions that are recovered in at least *J*% of the 'augmented ancestral networks' where *J* is the classification threshold maximizing the Youden's *J* statistic.

B-D: Estimates of the ancestral connectance (B), nestedness (C), and modularity (D) are represented at different times in the past (from 5 to 15 Myr ago) as a function of the simulated values. Each dot corresponds to one simulation, and for each simulation, we reported the estimated values averaged over 250 'augmented' ancestral networks. The black lines represent the line y=x, while the blue lines correspond to the fit of a linear model between the estimated and simulated values.

The figure reports results obtained for simulations under the scenario of evolution by anagenetic shifts (see Supplementary Figure 3 for other types of simulations).

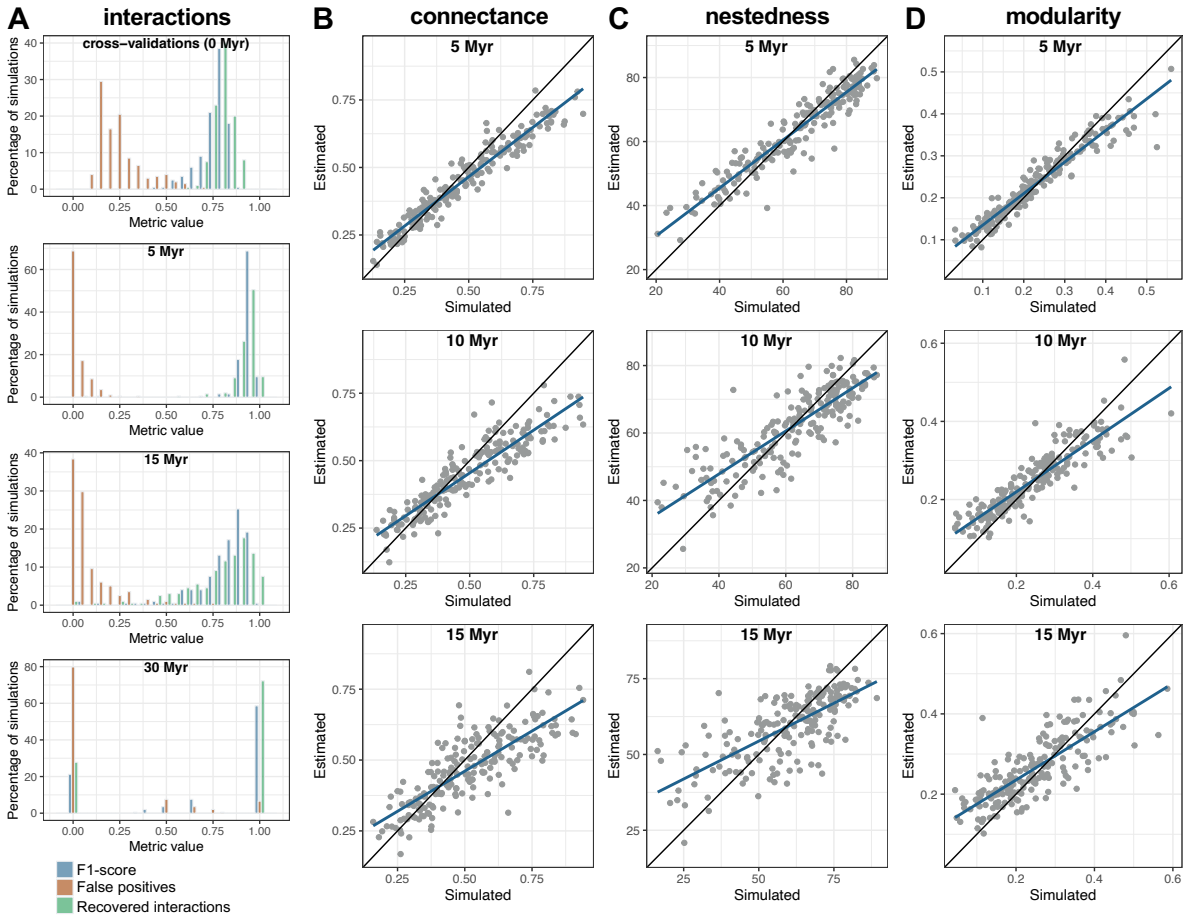

Our ancestral networks indeed reveal that angiosperms have preferentially formed associations with Glomeraceae, and non-angiosperms with early-diverging Glomeromycotina fungi, a pattern of phylogenetically structured modularity that has persisted since the origin of flowering plants (>150 Mya; Fig. 3A-C, Table S1). This tendency of flowering plants to interact with Glomeraceae ("recent plants with recent fungi") and non-flowering plants with non-Glomeraceae ("ancient plants with ancient fungi" (37)) has emerged more than 150 Myr, at the emergence of flowering plants, reinforcing the idea of an entangled diversification dynamic in these clades (38, 39). Similarly, phylogenetically structured modularity was already evident in bat pollination networks 10 Mya, corresponding to the divergence of bat subfamilies (Fig. 4). Compared with other mutualistic systems, seed dispersal networks exhibited elevated connectance (40), a pattern already present 10 Mya (Fig. 5A-B). Only a minority of taxa are specialists (Fig. 5C-D), yet the networks present a significant modularity, potentially shaped by phylogenetically conserved functional traits that mediate frugivory (41).

Figure 3: Global scale ancestral network reconstruction of arbuscular mycorrhizal symbiosis. Consensus ancestral networks 50 (A), 100 (B), or 130 (C) Myr ago. Ancestral network metrics (D). Squares indicate a significant departure from the null model (95% central range shown in orange), whereas the crosses indicate non-significance. Error bars represent the 95% central range of values obtained from the set of augmented ancestral networks.

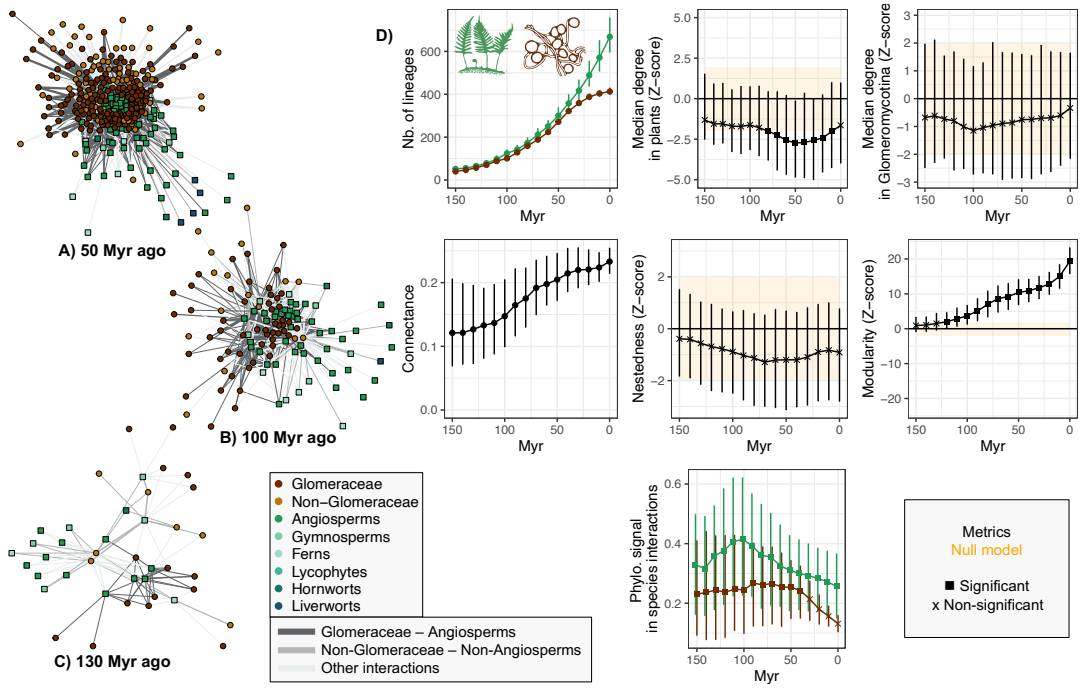

Figure 4: Ancestral network reconstruction of bat pollination in the Neotropics. Consensus ancestral network inferred 10 Myr ago (A). Ancestral network metrics (B). Squares indicate significant, and crosses non-significant departure from the null model (shown in orange), as in Fig. 3.

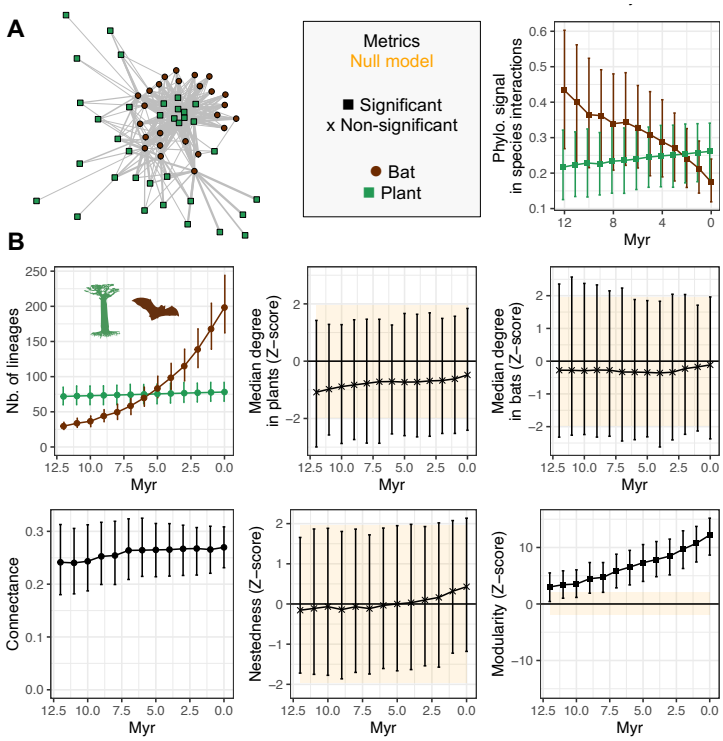

Figure 5: Ancestral network reconstruction of bird seed dispersal. Consensus ancestral networks inferred 10 Myr ago for the European (A) and American (B) bird seed dispersal networks. Ancestral network metrics (C & D). Squares indicate significant, and crosses non-significant departure from the null model (shown in orange), as in Fig. 3 & 4.

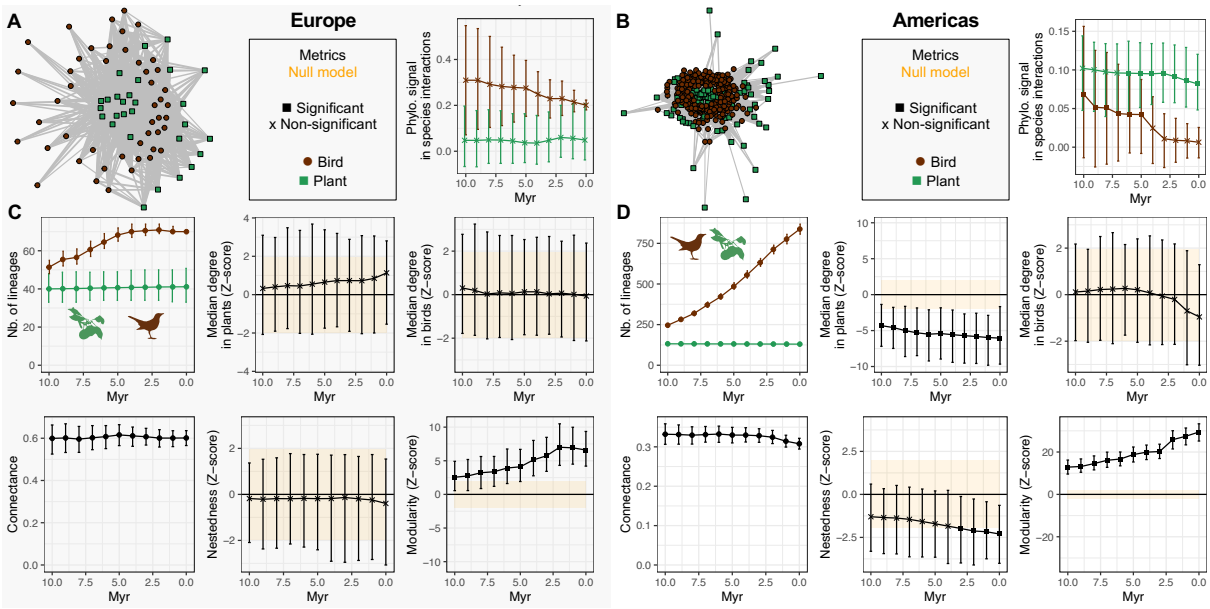

Discussion:

Present-day large-scale networks result from millions of years of coevolution among interacting species, but we lack direct observations of their deep-time evolution. We addressed this issue by developing a phylogenetic approach to reconstruct ancestral interaction networks. Ancestral continental and global networks of plant mutualisms involving arbuscular mycorrhizal fungi, bat pollinators, and bird seed dispersers show a consistent pattern of phylogenetically structured modularity that has persisted over macroevolutionary time scales.

The main idea underlying our approach, in comparison with previous attempts (27), is to introduce latent traits supposed to determine who interacts with whom, and to reconstruct these latent traits rather than directly the interactions. This is justified by the fact that interspecific interactions generally require a minimal level of compatibility between morphological, physiological, phenological, and/or behavioral traits to establish (1, 42). Hence, ideally, latent traits partially reflect biological traits that shape biotic interactions (4, 29). At the scales considered in the paper, latent traits may also reflect biogeography, which can constrain co-occurrence, and therefore potential interactions (43–45). We used a singular value decomposition of the present-day interaction matrix to estimate latent traits, following (29, 30). By construction, these latent traits are independent, determine different axes of variation in present-day interactions, and two species are more likely to interact if they exhibit high values for the same latent traits. While this interaction rule does not match traditional formulations of trait matching or phenotypic differences, we showed using simulations that the approach reliably recovers ancestral interactions across diverse simulated scenarios of network evolution when species interactions are evolutionary conserved, demonstrating the flexibility of latent traits in capturing who interacts with whom. We of course do not suggest that trait matching is not important in mutualism, but trait matching rules are often violated (e.g., small pollinators that do not use some flowers with short floral corolla, and to the contrary use flowers with long floral corolla tubes), such that a specific single-trait trait matching scenario is often biologically unrealistic. The latent trait approach provides an alternative, operational and more flexible way to characterize interactions.

The introduction of latent traits greatly simplifies the ancestral network reconstruction problem, as ancestral trait values can easily be obtained on the phylogenies of the interacting guilds under classical models of trait evolution. In addition, the

independency of the traits guaranteed by the singular value decomposition means that traits can be assumed to evolve independently. We used here independent Brownian motion processes, a general framework for trait evolution (46) that has previously been used to infer unknown present-day interactions (30). The Brownian process is prone to smoothing, which may explain the observed tendency towards homogenization of reconstructed ancestral networks. Other models of trait evolution could be used if more appropriate; for example, Ornstein-Uhlenbeck processes may better reflect processes of stabilizing selection and phenotypic convergence operating in mutualisms (6), and models with lineage-lineage trait coevolution (47) may better reflect the establishment of mutualistic syndromes – coevolved sets of complementary traits that tend to stabilize beneficial interactions – which are well-documented in the case of pollination (48). Future developments could also explicitly account for biogeographic range evolution and restrict potential interactions to species co-occurring in the same region (as, for example, in (49)).

Another strength of our approach is to explicitly account for extinct and unsampled lineages. While we found that our results are robust when not augmenting the trees, neglecting these missing lineages results in a large undersampling of past diversity, and could affect measures of ancestral network structure (50). We used here a constant-rate homogeneous birth-death model to complement the reconstructed phylogeny, but our framework could take advantage of recent developments that provide "augmented trees" under more realistic diversification models with heterogenous speciation and extinction rates through time and across lineages (35, 51). Considering "geographic" birth-death models, such as GeoSSE (52) or extensions (53) could in the future allow accounting for immigration and extirpation events that add or remove species from the geographic region considered, although such models have not yet been implemented with data augmentation. This step is necessarily imperfect given the current stage of development of phylogenetic diversification models, yet it is an improvement over ignoring missing lineages in phylogenies altogether.

Despite the flexibility of our approach, its performances vary: It performs best when modifications in the interactions occur anagenetically rather than cladogenetically, and when interactions are evolutionary conserved. When frequent interaction shifts occur, ancestral species are often inferred to interact while they do not (Fig. S3). Our simulations obviously do not (and cannot) cover all the processes known to play a role in the evolution of mutualisms, such as convergence (9). Yet they mimic diverse scenarios that cover the range of evolutionary conservatism expected in nature,

366 thereby allowing us to draw conclusions beyond the specific scenarios considered. For
367 example, we can expect the approach to perform well even in the presence of
368 convergence, if this convergence does not entirely erase phylogenic signal, and to not
369 perform well in the opposite case. Although this is typically not known *a priori* for a
370 given empirical system, our cross-validation procedure provides a general and robust
371 method for assessing the reliability of the ancestral reconstructions for any empirical
372 system. If the cross-validation F1-score falls below 0.25, mutualistic interactions may
373 be too evolutionarily labile or too strongly shaped by convergent evolution to be
374 reliably inferred in the past using ELEFANT. If the score exceeds 0.25, the
375 reconstructions can be trusted. In this case, we found that F1-scores of ancestral
376 interactions in the recent past were above 0.5. It may *a priori* seem surprising to find
377 better F1-scores in the recent past than in the present, but this is in fact expected from
378 the phylogenetic reconstruction, as estimates for "recent" internal nodes benefit from
379 more direct observed information (from their descendants) than phylogenetic tips. The
380 estimates are however less precise as we go deeper into the past, as in all ancestral
381 reconstruction techniques. As a rule of thumb, we would not consider ancestral
382 networks constructed past halfway through the clade's age to be reliable.
383
384 The global or continental ancestral networks of plant-mycorrhizal, pollination, and
385 seed dispersal mutualisms reveal a remarkably stable modular structure in the last
386 millions of years, despite continual changes in species composition driven by
387 speciation and extinction, and variations in environmental conditions. These results
388 were obtained by considering plants at the family level, given scarce interaction data
389 at the species level and computational limitations. We did run the analyses at the plant
390 species level for the small, well-sampled bat pollination network, and obtained
391 qualitatively similar results (not shown). This suggests that our conclusions may be
392 robust to the taxonomic level at which plants are considered, although this would need
393 to be confirmed. The stable modularity we reported in all plant mutualisms is
394 phylogenetically structured, with closely related species interacting with subsets of
395 closely-related partners. Such cophylogenetic signal (*sensu* (43)) has been reported
396 previously (42), but we show here that it is an evolutionarily stable characteristic of
397 these mutualistic networks, rather than a feature that emerged only recently. The
398 structural characteristics of local mutualistic networks, which tend to be more nested
399 (5) and to exhibit moderate phylogenetic signal (41, 54), may be quite different and
400 potentially less evolutionary stable. At large geographic scales, our results suggest that
401 selection favors the retention of existing beneficial associations over
402 macroevolutionary time scales (18), even if biogeographic barriers may also play a role.

This in turn may favor diffuse coevolution, reinforcing reciprocal specialization and compartmentalization (19). The extent to which the latent traits inferred by ELEFANT correspond to mutualistic syndromes could be investigated in the future (48). Our findings provide further support for the stability of mutualisms across macroevolutionary timescales associated with niche conservatism in species interactions (15, 23, 32). Such evolutionary stability of mutualistic network structure over millions of years now stands in sharp contrast to its rapid erosion under human pressures, which are driving an unprecedented, worldwide homogenization of ecological communities (10, 55).

By reconstructing ancestral networks, we can follow Darwin's 'entangled bank' through deep time. Tracing back the mutualistic side of this entangled bank suggests that the benefits of retaining established mutualistic relationships outweigh its costs, resulting in stable modules of closely-related species. Similar analyses of the antagonistic side may reveal much more instability, with Red Queen dynamics driving frequent partner shifts. This deep-time perspective on interspecific interactions lays the groundwork for understanding their role in species diversification – that is, how the entangled bank modulates global biodiversity patterns.

421 **Methods:**

422

423 **The ELEFANT model**

424

425 We consider two interacting guilds composed of h plant and p mutualist species
426 sampled at present ('plants' and 'mutualists' are used here for simplicity, but our
427 approach applies to any interacting groups of organisms, including antagonistic
428 interactors). The binary matrix $N\ (h, p)$ indicates whether each pair of plant and
429 mutualist species interact (1) or not (0). The extant, sampled species of each guild have
430 an associated reconstructed, time-calibrated phylogeny. We developed a framework,
431 the "Evolution of LatEnt traits For Ancestral NeTwork reconstruction" (ELEFANT),
432 illustrated in Fig. 1 and detailed in the next paragraphs, that infers ancestral network
433 from these combined network and phylogenetic data. The framework proceeds in five
434 steps, described below.

435

436 **i) Inferring present-day latent traits:**

437

438 First, assuming that interactions are shaped by unobserved traits, we obtain the
439 theoretical values of these latent traits for each extant species using the random dot
440 product graph (RDPG) method (29, 30)(Fig. 1.1). In previous developments, the
441 approach was used to infer present-day interactions of species for which interacting
442 partners were not known by inputting latent trait values to extant species, *i.e.*
443 phylogenetic tips (30, 36). Here, we aim to infer ancestral interactions. This method
444 performs a singular value decomposition of the present-day interaction matrix N by
445 finding the matrix $\Sigma\ (h, p)$ with null non-diagonal elements, and the matrices $L\ (h, h)$
446 and $R\ (p, p)$, such that $N = L \times \Sigma \times R^t$. Each diagonal element of the Σ matrix
447 corresponds to a singular value associated with a given share of the variance observed
448 in present-day interactions. By construction, these singular values are independent
449 and each of them defines an independent axis of variation of a latent trait. We selected
450 the d first eigenvalues ($\Sigma|d$) that explain at least 90% of the total variance observed in
451 present-day interactions. The values of the d independent latent traits associated to the
452 h plants are given by the $h \times d$ matrix $\tilde{L} = (L|d)$, and those associated to the p
453 mutualist s are given by the $d \times p$ matrix $\tilde{R} = (R|d)^t$. Each species is thus characterized
454 by a vector of d latent trait values. The interaction matrix N is approximated by $\tilde{L} \times$
455 $\Sigma|d \times \tilde{R}$. Thus, the sum of the products of each latent trait between plant i and
456 mutualist j, $\tilde{L}_i \times \Sigma|d \times \tilde{R}_j$, reflects their likelihood of interaction. In other words, the
457 probability of interaction between two species increases when both species exhibit

high values for the same latent traits. Consequently, specialist species tend to have on average lower latent trait values, whereas generalist species tend to have higher latent trait values. To determine the threshold J above which we can consider that there is an interaction between two species, we use a binary classification approach between the observed interaction network (N) and its approximation ($\widetilde{L} \times \Sigma | d \times \widetilde{R}$) (56): we take the J value maximizing the Youden's J statistic, defined as J = sensitivity (percentage of interactions correctly identified) + specificity (percentage of non-interactions correctly identified) – 1. This value is thus specific to each network. Other thresholds yielded similar results, with Youden's J threshold providing a good compromise (Fig. S3).

ii) Augmenting phylogenetic trees:

The second step (Fig. 1.2) is required to account for lineages that were likely involved in ancestral interactions but are missing in reconstructed trees, which lack all the lineages that left no descendants at present, either because they went extinct or were not sampled. For simplicity, we consider that the plant and mutualist phylogenies represent the diversification of two clades that follow each a constant-rate, homogeneous birth-death process, and we implement a data augmentation approach to simulate extinct and unsampled lineages on the plant and mutualist phylogenetic trees. Given the speciation rate λ, the extinction rate μ, and the sampling fraction at present ρ, all three assumed to be constant and known (in practice, λ and μ are estimated by maximum likelihood), we augment the phylogenetic trees with extinct and unsampled lineages (see Supplementary Methods). We account for stochasticity by independently replicating this data augmentation step 250 times. In the following steps, we thus work with a set of 'augmented' phylogenetic trees for each clade, which represent probable diversification histories. The assumption that the phylogenies on each side of the network represent the diversification of two clades following each a birth-death process corresponds best to a scenario where diversification occurs *in situ* at the spatial scale of the network, as in large (continental to global scale) networks over short enough timescales, or in close communities of *in situ* radiations, such as those found on remote islands or lakes. The assumption of a constant-rate homogeneous process can be relaxed with existing phylogenetic diversification models implemented with data augmentation (35, 51).

496 **iii) Inferring ancestral latent traits:**
497
498 Next, for each pair of plant and mutualist augmented trees, we perform ancestral state
499 reconstructions to estimate the latent trait values of each lineage back in time (Fig. 1.3).
500 We assume that the d latent traits of the plants ($\widetilde{L}$) and their mutualists ($\tilde{R}$) evolved
501 according to independent Brownian motion processes. For each latent trait, we infer
502 the parameters of the Brownian motion process using maximum likelihood (function
503 mvBM in the mvMORPH R-package (57)). Then, at each time point on the augmented
504 phylogenetic trees, we determine the expected value of each latent trait and their
505 variances (58, 59) and perform 250 stochastic character mappings.
506
507 **iv) Inferring ancestral networks:**
508
509 In the fourth step, we reconstruct the ancestral network $N(t)$ between coexisting
510 species at any given time t in the past (Fig. 1.4), based on the likelihood that two
511 species interact given their inferred latent trait values $N(t) \sim \widetilde{L}\,(t) \times\ \Sigma|d\ \times \tilde{R}(t)$ and
512 according to Youden's J threshold (see above). In the case of obligatory interactions,
513 where a species cannot survive without at least one partner, we force every species to
514 form at least one ancestral interaction: if the Youden's statistic is not reached with any
515 partner, we choose the partner species with the highest likelihood of interaction. This
516 only happens in a limited number of cases (<2% of the species in the empirical
517 applications).
518
519 **v) Cross-validations:**
520
521 The last step of ELEFANT aims to provide a measure of confidence in the ancestral
522 network reconstructions, given the strong assumptions made throughout: i)
523 interactions determined by latent traits derived from a truncated singular value
524 decomposition at present, ii) latent traits evolving according to independent Brownian
525 motion processes, and iii) latent traits, and therefore interactions, inherited at
526 speciation. We use cross-validation on the observed present-day interaction data to
527 obtain a measure of confidence in our model predictive accuracy (Fig. 1.5): we
528 randomly subsample 90% of the extant species, predict the partners of the other 10%,
529 repeat this procedure 100 times, and compute the average F1-score, defined as the
530 harmonic mean of the sensitivity (percentage of interactions correctly recovered) and
531 the precision (the ratio of recovered interactions corresponding to true interactions).
532 Based on the results obtained with simulations (Fig. S2), we consider reconstructions

reliable when the F1-score exceeds 0.25. Although this threshold may appear low, it reflects the intrinsic difficulty of our cross-validation design, in which ELEFANT must reconstruct ancestral interactions from present-day sampled species and subsequently predict present-day interactions of unsampled species from those ancestral reconstructions – that is, present to past to present. By contrast, the primary application of ELEFANT involves the reconstruction of ancestral interactions from present-day data (present to past), a task that consistently yields substantially higher F1-scores and thus greater reliability (see simulation results in Fig. 2D and Supplementary Figures).

Taking as input an interaction matrix (the network) and associated time-calibrated phylogenies, ELEFANT thus outputs at each time *t* in the past a set of 'augmented' ancestral networks representing probable interactions between both lineages present in the phylogeny and augmented lineages, as well as a measure of confidence in these reconstructions. When the two phylogenetic trees have different ages, ELEFANT provides reconstructions until the most recent common ancestor of the youngest clade.

Summarizing ancestral networks:

We summarized the structure of augmented ancestral networks by reporting several global metrics: i) species degrees, *i.e.* the average number of mutualists interacting with each plant and *vice-versa*, ii) connectance (the ratio of realized interactions), iii) nestedness (the tendency of specialist species to interact with generalist partners, measured using the NODF2 index (60)), iv) modularity (the percentage of interactions belonging to subsets of species preferentially interacting together – computed using the function computeModules (60)), and v) the phylogenetic signal of species interactions in each guild, *i.e.*, the tendency of closely related species to interact with similar partners, measured using Mantel tests (61).

We also generated consensus ancestral networks constituted of frequently recovered interactions between pairs of species (28). We added an interaction in the consensus network if it was recovered in at least x% of the augmented ancestral networks, with x being either 10%, 25%, 50%, or *J*% (Youden's *J* threshold). Consensus networks do not contain interactions involving augmented species, are these vary across augmented trees.

570 **Simulations**

571

572 We evaluated the ability of ELEFANT to reconstruct ancestral networks thanks to five
573 simulated scenarios. We designed them based on different assumptions about how
574 interaction networks could evolve, with the aim to obtain realistic simulated networks
575 that resemble empirical ones. Although additional, more specialized simulations
576 could have been developed—for example, incorporating convergent evolution in
577 mutualisms, codiversification, mass extinction events, or preferential extinctions of
578 key hub species —our goal was not to exhaustively test ELEFANT across all possible
579 modes of mutualism evolution. Instead, we sought to characterize its performance
580 under a range of scenarios differing in the degree of evolutionary conservatism of
581 species interactions (see below). For systems in which ongoing processes not
582 represented in our simulations are suspected (e.g. convergent evolution), the cross-
583 validation procedure (see above) provides a way to assess the ability of ELEFANT to
584 recover subsampled interactions directly from the empirical dataset, without requiring
585 additional simulations.

586

587 As in the main text, we use "plants" and "mutualists" to refer to the two interacting
588 guilds for simplicity and to match our empirical examples, but these simulations can
589 equally represent the evolution of any two interacting guilds, including those engaged
590 in antagonistic interactions.

591

592 In each of the five scenarios, we simulated network evolution for 30 million years and
593 recorded the simulated ancestral networks every 5 million years. Both the plants and
594 the mutualists diversified according to a constant rate birth-death process with a
595 speciation rate (λ) uniformly sampled between 0.05 and 0.2 and an extinction rate (μ)
596 between 0.01 and 0.05. For computational reasons, we only kept simulated systems
597 having between 25 and 150 extant species per guild. We generated a total of 200
598 simulations per scenario.

599

600 **i) Evolution by anagenetic shifts:**

601

602 We simulated the evolution of plant-mutualist interaction networks where the
603 mutualists are obligately associated with at least one plant species, while the plants
604 are only facultatively interacting with the mutualists (e.g. seeds can be dispersed by
605 mammals if they are not by birds). We started the process with the diversification of
606 plants, with that of the mutualists starting 10 million years after; we considered that

the most recent common ancestor of the mutualists interacted with one single plant lineage picked at random. Then, we assumed that interactions are inherited at speciation events (no cladogenetic changes, the two descendant lineages inherit the interacting partners of their ancestor) but can change during the life time of the lineages (anagenetic shifts): a mutualist lineage can acquire a new interaction with an additional plant species chosen at rate 0.015 (number of events Myr^{-1}), or lose one of the plant species it interacts with at a rate of 0.015. The plant partners that are gained or lost are picked at random. When a lineage goes extinct, the species it interacts with lose their partner. If this was the only interaction of the mutualist, a new interacting plant lineage is picked at random.

ii) Evolution by cladogenetic shifts:

By modeling the evolution of latent traits using Brownian motions, ELEFANT assumes that the latent trait values are inherited at speciation and therefore that the two daughter species are likely to keep the same interactions. However, there are examples of closely related species that likely switched partners at speciation (62, 63) and such cladogenetic shifts may not be well handled by ELEFANT. We therefore simulated a scenario where network evolution happened through both anagenetic and cladogenetic shifts. We built upon the scenario "evolution by anagenetic shifts" with a rate of anagenetic acquisition of 0.15 and a rate of anagenetic loss of 0.05 and added cladogenetic shifts. At each mutualist speciation event, one of the two daughter lineages retains the same interacting plant species, while the other daughter lineage forms an entirely new set of interactions with randomly selected plants.

iii) Brownian evolution of latent traits:

Next, we considered one simulated scenario corresponding to the underlying model of ELEFANT. We simulated the independent evolution of d=10 latent traits using Brownian motions on the plant and mutualist phylogenetic trees with 0 as ancestral values and a variance of 0.01. We attributed interactions between pairs of plant and mutualist species if the product of their latent traits was larger than 0.25. Both plant and mutualist species were considered to be obligatory partners.

iv) Host repertoire evolution:

In this scenario, we assumed that host taxa (plants) diversified before the most recent common ancestor of the mutualists (*e.g.* it can correspond to higher taxonomic levels, *e.g.* plant families) and we tracked the set of host taxa associated with each mutualist species during their diversification. Following Braga *et al.* (27), we referred to this set of associated host taxa as the host repertoire. Each mutualist obligatorily interacts with at least one host taxon, while the hosts only facultatively interact with mutualists. We started the simulation by randomly attributing one host taxon to the most recent common ancestor of the mutualists. Then, the host repertoire of each mutualist lineage evolved independently by acquiring new host taxa at a rate of 0.15 and losing host taxa at a rate of 0.05 following a continuous-time Markov process. Host repertoires are inherited at mutualist speciation.

v) Random evolution:

Finally, we considered a scenario of fast interaction evolution where network evolution occurs by anagenetic shifts at very high rates, such that interspecific interactions are not conserved over macroevolutionary timescales. To simulate this scenario, we used the first simulation scenario with a rate of plant acquisition of 100 and a rate of plant loss of 200.

We assumed that not all extant species were sampled at present and used a sampling probability (ρ) uniformly sampled between 60% and 100%, as undersampling is a common phenomenon in empirical networks (50). We discarded extinct and unsampled species from the phylogenetic trees of each guild; we referred to these new trees as the 'reconstructed trees'. In addition, we considered that not all interactions are sampled at present and that present-day interactions between sampled species have only a 90% chance of being observed while keeping at least one observed interaction per species. We referred to these subsampled present-day networks as the 'observed networks'.

The values of the parameters used in the different simulations were chosen to obtain a range of realistic simulated networks mimicking the variability observed in empirical ones. Indeed, we obtained ranges of size, connectance, modularity, and nestedness values comparable to those of empirical networks (Fig. S4)(40). We also obtained a

range of phylogenetic signals in species interactions (Supplementary Results, Fig. S8), with many networks showing low signals as often observed in nature (54).

We then ran ELEFANT on each simulation composed of one observed network and two reconstructed trees. For the step of data augmentation of extinct and unsampled lineages, we used the simulated parameters values λ, μ, and ρ, and generated a total of 250 augmented ancestral networks. Between 5 and 15 singular values were often necessary to explain at least 90% of the present-day interactions in the different types of simulated networks (Supplementary Results; Fig. S9).

We then compared the simulated *versus* inferred global metrics of the ancestral networks (number of species, connectance, nestedness, and modularity) by fitting linear models. We also evaluated whether the analyses recovered significant phylogenetic signals when present in the simulations. Finally, we looked at the inferred ancestral interactions present in the consensus ancestral networks and reported the sensitivity (percentage of interactions correctly identified), the percentage of interactions corresponding to false positives, and the corresponding F1-score. We replicated the analyses without data augmentation (μ=0 and ρ=1) and confirmed that adding extinct and unsampled lineages significantly increased the performance of ELEFANT (Supplementary Results; Fig. S10).

The implementation of ELEFANT and all simulations were performed in R (64).

Empirical applications

We applied ELEFANT to three different mutualistic systems involving plants and covering a broad range of temporal and spatial scales: the global-scale arbuscular mycorrhizal symbiosis, the pollination by bats in the Neotropics, and the seed dispersal by birds in Europe and the Americas. Although we presented ELEFANT as a species-level model applied to monophyletic clades, it can technically be applied at any taxonomic level (*e.g.* genus or family), and to non-monophyletic groups of organisms, as long as the taxa included in the network and in the phylogenetic trees match. Here, in order to reduce "missing" data (e.g. plant species which mycorrhizal partners have not been characterized) and better match the type of network structures obtained in our simulations, we considered plants at the family level. In addition, plant mutualists correspond to ecologically- and/or geographically-defined groups of taxa (*e.g.* nectar feeding bats, bird seed dispersers in Europe). The "augmentation" step of

718 the framework should thus be considered as an imperfect attempt to account for
719 missing lineages, rather than as a rigorous reconstruction of past diversification and
720 diversity histories (as, in, *e.g.* (35, 51)). For example, the birth-death model is not ideal
721 to represent the (dis)appearance of higher taxa (see, *e.g.* (65) for a better model), and
722 only makes sense in the case of ecologically- and/or geographically-defined groups of
723 taxa for which it can be assumed that ecological and/or geographical transitions have
724 been rare in the time period over which networks are reconstructed. We limited our
725 continental-scale reconstructions (for bats and birds) to relatively recent time periods
726 (on the order of 10 Myr), on which the latter assumption is reasonable. This does
727 exclude the possibility that important immigration events occurred (for example, the
728 thrushes arrived in the Americas between 11 and 4 million years ago, (66)), but these
729 rare events are unlikely to deeply affect the global structure of ancestral networks.
730 Given these imperfections in the reconstruction of ancestral lineages, which could
731 affect the reconstruction of ancestral networks, we assess the robustness of our results
732 to choices made during the data augmentation step.
733
734 First, we reconstructed ancestral interaction networks of the arbuscular mycorrhizal
735 symbiosis between land plants and Glomeromycotina fungi at the global scale. We
736 gathered the interaction data from the MaarjAM database ((67); https://maarjam.ut.ee)
737 filtered according to (12). We considered the network at the levels of virtual taxa (VT)
738 for the Glomeromycotina (391 taxa delimited using DNA-based criteria; (67)) and
739 plant families (115 families). We used a phylogenetic tree of Glomeromycotina from
740 (38) and reconstructed the plant phylogeny by pruning the mega-tree of vascular
741 plants using V-PhyloMaker2 (68). We ran ELEFANT with λ=0.012, μ=0.001, and ρ=0.86
742 for Glomeromycotina following the estimates of (38), and λ=0.02, μ=0.003, and ρ=0.19
743 for the plants (the two former parameters were estimated by fitting a constant-rate
744 birth-death model in RPANDA on the family-level phylogeny of land plants (69) with
745 a sampling fraction computed as the number of sampled plant families (115) divided
746 by the estimated total number of plant families (600)). We looked at the ancestral
747 networks for the past 150 Myr, which corresponds to the emergence of Angiosperms,
748 and respects the "halfway through clades age" rule of thumb.
749
750 Second, we investigated the evolution of plant-bat pollination networks. We gathered
751 the interaction data from (70). We focused our analysis on the evolution of nectar-
752 feeding bat pollinators from the Phyllostomidae family, a Neotropical bat family
753 including many nectar-feeding species. We obtained the phylogenetic tree of the 56
754 bat species from (71) and used V-PhyloMaker2 for the phylogenetic tree of the 42 plant

755 families. We ran ELEFANT with λ=0.20, μ=0.01 (71), and ρ=0.31 for the bats (obtained
756 by assuming that there are 180 extant species of the nectar-feeding Phyllostomidae
757 family (72)) and λ=0.02, μ=0.003, and ρ=0.63 for the bat-pollinated plants (73). We
758 looked at the ancestral networks for the past 12 Myr, which is less than half the age of
759 the Phyllostomidae family.
760
761 Third, we studied seed dispersal of fleshy fruits by birds in Europe and the Americas.
762 We obtained the plant-bird interactions from (10), the bird phylogenetic tree from (74),
763 and the plant phylogenetic tree from V-PhyloMaker2. Europe and Americas were
764 picked as they formed two well-sampled, separated modules in the global-scale
765 network of seed dispersal by birds (10). In Europe, the network contained 70 bird
766 species and 28 plant families forming fleshy fruits, with sampling fractions (ρ) of 1 and
767 0.78, respectively (75, 76). In the Americas, it contained 586 bird species and 115 plant
768 families forming fleshy fruits, with sampling fractions (ρ) of 0.73 and 0.93, respectively
769 (75). We ran ELEFANT with λ=0.15 and μ=0.01 for the birds (77) and λ=0.02 and μ=0.003
770 for the plants. We looked at the ancestral networks for the past 10 Myr, which limited
771 the number of potential bird immigration events while still encompassing a significant
772 number of speciation events.
773
774 The three empirical networks showed different levels of phylogenetic signal. In the
775 arbuscular mycorrhizal symbiosis, significant signal was detected in both plants
776 (R=0.30, p<0.001) and fungi (R=0.11, p<0.001). Similarly, the pollination network
777 exhibits significant phylogenetic signal in both plants (R=0.13, p=0.01) and bats
778 (R=0.12, p<0.001). In contrast, in the European seed dispersal network, closely related
779 birds interact with similar plant families (R=0.21, p<0.01), but not the reverse (R=-0.01,
780 p=0.50), and no significant signal was observed in the American seed dispersal
781 network (p-values>0.05). In these mutualistic networks, respectively, 38, 12, 4, and 18
782 latent traits were necessary to explain at least 90% of the present-day interactions.
783
784 To evaluate the significance of the structural properties of the ancestral networks
785 (nestedness, modularity, and phylogenetic signals), we compared the original metrics
786 with that obtained under a null model. Following (28), for each augmented ancestral
787 network, we used the "r00" null model (function *nullmodel* in the R-package vegan),
788 which randomizes the interactions while maintaining the network connectance. To
789 evaluate the robustness of our results, we reran ELEFANT without using data
790 augmentation or with other rates of diversification for the step of data augmentation
791 (Table S2; Fig. S7).

Acknowledgments:

The authors acknowledge G. Dalla Riva for helpful discussions of the RDPG methods as well as the members of the 'Modeling Biodiversity' team at IBENS for constructive feedbacks.
This work was performed using HPC resources from GENCI-IDRIS (Grant 2022-AD010313735).

Data availability:

All the functions developed for running ELEFANT are available on GitHub: https://github.com/BPerezLamarque/ELEFANT
All scripts and empirical data used in this manuscript are available on OSF with the following DOI: https://doi.org/10.17605/OSF.IO/K275U

References:

1. J. L. Bronstein, *Mutualism*, J. L. Bronstein, Ed. (Oxford University Press, 2015) https:/doi.org/10.1093/acprof:oso/9780199675654.001.0001 (December 12, 2018).
2. D. H. Hembry, M. G. Weber, Ecological interactions and macroevolution: A new field with old roots. *Annu. Rev. Ecol. Evol. Syst.* **51**, 215–243 (2020).
3. L. J. Harmon, *et al.*, Detecting the macroevolutionary signal of species interactions. *J. Evol. Biol.* **32**, 769–782 (2019).
4. J. Bascompte, P. Jordano, *Mutualistic networks* (Princeton University Press, 2013).
5. E. Thébault, C. Fontaine, Stability of ecological communities and the architecture of mutualistic and trophic networks. *Science (80-.).* **329**, 853–856 (2010).
6. O. Maliet, N. Loeuille, H. Morlon, An individual based model for the eco-evolutionary emergence of bipartite interaction networks. *Ecol. Lett.* **23**, ele.13592 (2020).
7. C. Fontaine, *et al.*, The ecological and evolutionary implications of merging different types of networks. *Ecol. Lett.* **14**, 1170–1181 (2011).
8. M. A. Fortuna, *et al.*, Nestedness versus modularity in ecological networks: Two sides of the same coin? *J. Anim. Ecol.* **79**, 811–817 (2010).
9. C. I. Donatti, *et al.*, Analysis of a hyper-diverse seed dispersal network: Modularity and underlying mechanisms. *Ecol. Lett.* **14**, 773–781 (2011).
10. E. C. Fricke, J. Svenning, Accelerating homogenization of the global plant – frugivore meta-network. *Nature* **585** (2020).
11. J. Davison, *et al.*, Global assessment of arbuscular mycorrhizal fungus diversity

reveals very low endemism. *Science (80-.).* **349**, 970–973 (2015).
12. B. Perez-Lamarque, M. A. Selosse, M. Öpik, H. Morlon, F. Martos, Cheating in arbuscular mycorrhizal mutualism: a network and phylogenetic analysis of mycoheterotrophy. *New Phytol.* **226**, 1822–1835 (2020).
13. T. Poisot, D. Stouffer, How ecological networks evolve. *bioRxiv*, 071993 (2016).
14. S. T. Segar, *et al.*, The role of evolution in shaping ecological networks. *Trends Ecol. Evol.* **35**, 454–466 (2020).
15. G. Burin, P. R. Guimarães, T. B. Quental, Macroevolutionary stability predicts interaction patterns of species in seed dispersal networks. *Science (80-.).* **372**, 733–737 (2021).
16. J. L. Bronstein, The study of mutualism, past, present, and future. *Am. Nat.* **in press.** (2025).
17. M. P. Braga, P. R. Guimarães, C. W. Wheat, S. Nylin, N. Janz, Unifying host-associated diversification processes using butterfly–plant networks. *Nat. Commun.* **9**, 5155 (2018).
18. P. R. Guimarães, P. Jordano, J. N. Thompson, Evolution and coevolution in mutualistic networks. *Ecol. Lett.* **14**, 877–885 (2011).
19. J. M. Olesen, J. Bascompte, Y. L. Dupont, P. Jordano, The modularity of pollination networks. *Proc. Natl. Acad. Sci.* **104**, 19891–19896 (2007).
20. M. L. Stanton, Interacting guilds: Moving beyond the pairwise perspective on mutualisms in *American Naturalist*, (2003), pp. S10–S23.
21. J. N. Thompson, B. M. Cunningham, Geographic structure and dynamics of coevolutionary selection. *Nature* **417**, 735–738 (2002).
22. J. Genini, L. P. C. Morellato, P. R. Guimarães, J. M. Olesen, Cheaters in mutualism networks. *Biol. Lett.* **6**, 494–497 (2010).
23. J. M. Gómez, M. Verdú, F. Perfectti, Ecological interactions are evolutionarily conserved across the entire tree of life. *Nature* **465**, 918–921 (2010).
24. J. A. Dunne, R. J. Williams, N. D. Martinez, R. A. Wood, D. H. Erwin, Compilation and network analyses of Cambrian food webs. *PLoS Biol.* **6**, 693–708 (2008).
25. J. C. S. Nascimento, F. Blanco, M. S. Domingo, J. L. Cantalapiedra, M. M. Pires, The reorganization of predator–prey networks over 20 million years explains extinction patterns of mammalian carnivores. *Ecol. Lett.* **27**, e14448 (2024).
26. M. J. Landis, N. J. Matzke, B. R. Moore, J. P. Huelsenbeck, Bayesian analysis of biogeography when the number of areas is large. *Syst. Biol.* **62**, 789–804 (2013).
27. M. P. Braga, M. J. Landis, S. Nylin, N. Janz, F. Ronquist, Bayesian inference of ancestral host-parasite interactions under a phylogenetic model of host repertoire evolution. *Syst. Biol.* **69**, 1149–1162 (2020).
28. M. P. Braga, N. Janz, S. Nylin, F. Ronquist, M. J. Landis, Phylogenetic reconstruction of ancestral ecological networks through time for pierid butterflies and their host plants. *Ecol. Lett.* **24**, 2134–2145 (2021).
29. G. V. Dalla Riva, D. B. Stouffer, Exploring the evolutionary signature of food webs' backbones using functional traits. *Oikos* **125**, 446–456 (2016).

30. T. Strydom, *et al.*, Food web reconstruction through phylogenetic transfer of low-rank network representation. *Methods Ecol. Evol.* **2022**, 1–12 (2022).
31. M.-A. Selosse, F. Le Tacon, The land flora: a phototroph-fungus partnership? *Trends Ecol. Evol.* **13**, 15–20 (1998).
32. Y. Zeng, J. J. Wiens, Do mutualistic interactions last longer than antagonistic interactions? *Proc. R. Soc. B Biol. Sci.* **288** (2021).
33. D. Peris, *et al.*, Evolutionary implications of a deep-time perspective on insect pollination. *Biol. Rev.* **100**, 1452–1466 (2025).
34. S. L. Nuismer, L. J. Harmon, Predicting rates of interspecific interaction from phylogenetic trees. *Ecol. Lett.* **18**, 17–27 (2015).
35. O. Maliet, H. Morlon, Fast and accurate estimation of species-specific diversification rates using data augmentation. *Syst. Biol.* **71**, 353–366 (2022).
36. F. Massol, E. Macke, M. Callens, E. Decaestecker, A methodological framework to analyse determinants of host–microbiota networks, with an application to the relationships between Daphnia magna's gut microbiota and bacterioplankton. *J. Anim. Ecol.* **90**, 102–119 (2021).
37. W. R. Rimington, S. Pressel, J. G. Duckett, K. J. Field, M. I. Bidartondo, Evolution and networks in ancient and widespread symbioses between Mucoromycotina and liverworts. *Mycorrhiza* **29**, 551–565 (2019).
38. B. Perez-Lamarque, *et al.*, Analysing diversification dynamics using barcoding data: The case of an obligate mycorrhizal symbiont. *Mol. Ecol.* **31**, 3496–3512 (2022).
39. F. Lutzoni, *et al.*, Contemporaneous radiations of fungi and plants linked to symbiosis. *Nat. Commun.* **9**, 1–11 (2018).
40. B. Pichon, R. Le Goff, H. Morlon, B. Perez-Lamarque, Telling mutualistic and antagonistic ecological networks apart by learning their multiscale structure. *Methods Ecol. Evol.* **15**, 1113–1128 (2024).
41. L. Fuzessy, M. Verdú, M. A. Pizo, Ecological function over evolutionary legacy: The limited role of shared evolutionary history in shaping modern frugivory interactions. *Funct. Ecol.* **00**, 1–16 (2025).
42. E. L. Rezende, P. Jordano, J. Bascompte, Effects of phenotypic complementarity and phylogeny on the nested structure of mutualistic networks. *Oikos* **116**, 1919–1929 (2007).
43. B. Perez-Lamarque, H. Morlon, Distinguishing cophylogenetic signal from phylogenetic congruence clarifies the interplay between evolutionary history and species interactions. *Syst. Biol.* **73**, 613–622 (2024).
44. F. Encinas-Viso, T. A. Revilla, R. S. Etienne, Phenology drives mutualistic network structure and diversity. *Ecol. Lett.* **15**, 198–208 (2012).
45. M. A. R. Mello, *et al.*, Insights into the assembly rules of a continent-wide multilayer network. *Nat. Ecol. Evol.* **3**, 1525–1532 (2019).
46. L. J. Revell, L. J. Harmon, D. C. Collar, Phylogenetic signal, evolutionary process, and rate. *Syst. Biol.* **57**, 591–601 (2008).
47. M. Manceau, A. Lambert, H. Morlon, A unifying comparative phylogenetic

framework including traits coevolving across interacting lineages. *Syst. Biol.* **66**, 551–568 (2017).
48. C. B. Fenster, W. S. Armbruster, P. Wilson, M. R. Dudash, J. D. Thomson, Pollination syndromes and floral specialization. *Annu. Rev. Ecol. Evol. Syst.* **35**, 375–403 (2004).
49. J. P. Drury, *et al.*, Contrasting impacts of competition on ecological and social trait evolution in songbirds. *PLoS Biol.* **16**, e2003563 (2018).
50. C. Llopis-Belenguer, *et al.*, Sensitivity of bipartite network analyses to incomplete sampling and taxonomic uncertainty. *Ecology* **104**, e3974 (2023).
51. I. Quintero, N. Lartillot, H. Morlon, Imbalanced speciation pulses sustain the radiation of mammals. *Science (80-.).* **384**, 1007–1012 (2024).
52. E. E. Goldberg, L. T. Lancaster, R. H. Ree, Phylogenetic inference of reciprocal effects between geographic range evolution and diversification. *Syst. Biol.* **60**, 451–465 (2011).
53. I. Quintero, M. J. Landis, W. Jetz, H. Morlon, The build-up of the present-day tropical diversity of tetrapods. *Proc. Natl. Acad. Sci.* **120** (2023).
54. E. L. Rezende, J. E. Lavabre, P. R. Guimarães, P. Jordano, J. Bascompte, Non-random coextinctions in phylogenetically structured mutualistic networks. *Nature* **448**, 925–928 (2007).
55. I. Junk, *et al.*, Archived natural DNA samplers reveal four decades of biodiversity change across the tree of life. *Nat. Ecol. Evol.*, 1–12 (2025).
56. T. Poisot, *et al.*, Network embedding unveils the hidden interactions in the mammalian virome. *Patterns* **4**, 100738 (2023).
57. J. Clavel, G. Escarguel, G. Merceron, mvMORPH: An R package for fitting multivariate evolutionary models to morphometric data. *Methods Ecol. Evol.* **6**, 1311–1319 (2015).
58. E. P. Martins, T. F. Hansen, Phylogenies and the comparative method: A general approach to incorporating phylogenetic information into the analysis of interspecific data. *Am. Nat.* **149**, 646–667 (1997).
59. J. Clavel, L. Aristide, H. Morlon, A penalized likelihood framework for high-dimensional phylogenetic comparative methods and an application to New-World monkeys brain evolution. *Syst. Biol.* **68**, 93–116 (2019).
60. C. F. Dormann, B. Gruber, J. Fründ, Introducing the bipartite package: analysing ecological networks. *R News* **8**, 8–11 (2008).
61. B. Perez-Lamarque, *et al.*, Do closely related species interact with similar partners? Testing for phylogenetic signal in bipartite interaction networks. *Peer Community J.* **2**, e59 (2022).
62. D. M. de Vienne, *et al.*, Cospeciation vs host-shift speciation: Methods for testing, evidence from natural associations and relation to coevolution. *New Phytol.* **198**, 347–385 (2013).
63. N. E. Langmore, *et al.*, Coevolution with hosts underpins speciation in brood-parasitic cuckoos. *Science (80-.).* **384**, 1030–1036 (2024).
64. R Core Team, R: A language and environment for statistical computing. (2024).

65. L. L. Sánchez-Reyes, H. Morlon, S. Magallón, Uncovering higher-taxon diversification dynamics from clade age and species-richness data. *Syst. Biol.* **66**, 367–378 (2017).
66. J. Nagy, Z. Végvári, Z. Varga, Phylogeny, migration and life history: filling the gaps in the origin and biogeography of the Turdus thrushes. *J. Ornithol.* **160**, 529–543 (2019).
67. M. Öpik, *et al.*, The online database MaarjAM reveals global and ecosystemic distribution patterns in arbuscular mycorrhizal fungi (Glomeromycota). *New Phytol.* **188**, 223–241 (2010).
68. Y. Jin, H. Qian, V.PhyloMaker2: An updated and enlarged R package that can generate very large phylogenies for vascular plants. *Plant Divers.* **44**, 335–339 (2022).
69. H. Morlon, *et al.*, RPANDA: An R package for macroevolutionary analyses on phylogenetic trees. *Methods Ecol. Evol.* **7**, 589–597 (2016).
70. K. González-Gutiérrez, J. H. Castaño, J. Pérez-Torres, H. R. Mosquera-Mosquera, Structure and roles in pollination networks between phyllostomid bats and flowers: a systematic review for the Americas. *Mamm. Biol.* **102**, 21–49 (2022).
71. N. S. Upham, J. A. Esselstyn, W. Jetz, Inferring the mammal tree: Species-level sets of phylogenies for questions in ecology, evolution, and conservation. *PLoS Biol.* **17**, e3000494 (2019).
72. T. Datzmann, O. Von Helversen, F. Mayer, Evolution of nectarivory in phyllostomid bats (Phyllostomidae Gray, 1825, Chiroptera: Mammalia). *BMC Evol. Biol.* **10**, 1–14 (2010).
73. T. H. Fleming, C. Geiselman, W. J. Kress, The evolution of bat pollination: a phylogenetic perspective. *Ann. Bot.* **104**, 1017–43 (2009).
74. W. Jetz, G. H. Thomas, J. B. Joy, K. Hartmann, A. O. Mooers, The global diversity of birds in space and time. *Nature* **491**, 444–448 (2012).
75. W. D. Kissling, K. Böhning-Gaese, W. Jetz, The global distribution of frugivory in birds. *Glob. Ecol. Biogeogr.* **18**, 150–162 (2009).
76. P. Vargas, R. Heleno, J. M. Costa, EuDiS - A comprehensive database of the seed dispersal syndromes of the European flora. *Biodivers. data J.* **11**, e104079 (2023).
77. O. Maliet, F. Hartig, H. Morlon, A model with many small shifts for estimating species-specific diversification rates. *Nat. Ecol. Evol.* **3**, 1086–1092 (2019).